

New Isolated Interface Converter for PMSG based Variable Speed Wind Turbines

Abstract. This paper presents a new converter topology for interfacing a permanent magnet synchronous generator based variable speed wind turbine with a residential power network. The theory of wind energy conversion is analyzed first. Then an example of wind velocity distribution and normalized energy yield is discussed in order to formulate requirements for choosing a power converter. A new topology of an interfacing converter is analyzed and simulation results of a lossless model are presented. Simulation and experimental results of the proposed converter prove that its utilization in wind power applications is beneficial.

Streszczenie. W artykule przedstawiono nową topologię przekształtnika do sprzęgania instalacji domowych z turbiną wiatrową o zmiennej prędkości zbudowaną na bazie generatora synchronicznego z magnesami trwałymi. W pierwszej kolejności przedstawiona została teoria przetwarzania energii wiatru. Następnie w celu sformułowania wymagań dotyczących wyboru mocy przekształtnika omówiono przykład rozkładu prędkości wiatru i znormalizowaną wydajność energetyczną. Nowa topologia przekształtnika sprzęgającego jest analizowana i symulowana przy założeniu modeli bezstratnych. Wyniki badań symulacyjnych i eksperymentalnych proponowanego przekształtnika udowodniły, że jego zastosowanie w elektrowniach wiatrowych jest korzystne. (Nowy izolowany sprzęt przekształtnikowy do turbin wiatrowych na bazie generatora PMSG).

Keywords: wind energy, PMSG, qZS DC/DC converter, variable speed wind turbines.

Słowa kluczowe: energia wiatru, PMSG, przekształtnik qZS DC/DC, turbiny wiatrowe o zmiennej prędkości.

Introduction

Sustainability is the main aspect that forces the renewable energy sources to be implemented for electric energy generation instead of fossil ones. Wind energy is quite attractive among other sources because of its commercial potential [72 TW] that is five times higher than world energy demand in all forms. However, the installed capacity in 2009 was only 159GW [1] and [2]. Large turbines play a main role on the market, but there is also demand for small turbines in the power range up to 11 kW as the power source for micro generators.

Micro generator is an electrical energy source that includes all interface units and operates in parallel with the distribution network. Current rating of such devices is limited up to 16 A per phase [3]. Some energy sources can be connected directly to the distribution network, but in the case of DC power sources or variable speed wind turbine (VSWT) systems it is necessary to use a power converter that interfaces the source and the grid.

VSWT based micro generators consist of a wind turbine, a generator and an inverter. Wind turbines capture wind energy and convert it to rotational mechanical energy. Variable speed operation of the wind turbine allows extraction of higher energy from wind than constant speed systems [4]. The generator converts mechanical energy into electricity. Different types of generators can be used in wind energy conversion systems (WECS), but permanent magnet synchronous generators (PMSG) play a main role on the market [5]. The main advantage of PMSG is the possibility of multipole design that offers slow speed operation and the possibility of gearless WECS construction. Another advantage is maintenance free operation since there are no brushes. The main drawback of PMSG is the dependence of its output voltage on the rotation speed. The difference between the minimum and the maximum voltage can reach four times in VSWT applications [3]. This drawback can be easily overcome with the help of an appropriate interfacing converter.

The interfacing converter rectifies the input AC with variable voltage and frequency, adjusts voltage levels and inverts DC voltage into AC with grid voltage and frequency. Additionally, it should have maximum power point tracking (MPPT) functionality to extract more power from wind. Different topologies of the interfacing converter are discussed in the literature [4-18]. Basically they can be

divided into two groups: topologies without galvanic isolation [16] (Fig. 1a) and those with isolation. Line frequency (LF) transformers (Fig. 1b) were widely used for galvanic isolation in last decades [9]. Main drawbacks of LF transformer are high weight and high price. For these reasons topologies with HF isolation (Fig. 1c) have become popular especially for photovoltaic applications [15], but there are only few topologies for wind applications studied in the literature [10,15].

All the topologies mentioned have a distinct DC link. It means that on the generator side there is a rectifier, but an inverter is placed on the grid side. Some low pass filter can be added to the inverter to fulfil standard requirements. Inverters have full bridge configuration in most cases because of lower DC link voltage. Since the inverter is well-known, this part of the interfacing converter would not be investigated in this paper.

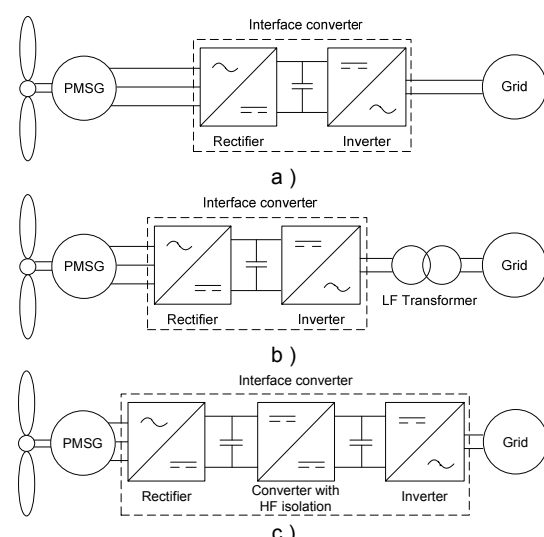


Fig.1. Block diagrams of interface converters

The basic function of a rectifier is input voltage rectification, but it can ensure additional functions: power factor correction (PFC), DC link voltage stabilization and MPPT. Three-phase diode rectifiers are used in simple systems [11]. This configuration with diode rectifier is not suitable for VSWT since it cannot ensure necessary DC

voltage level in all wind conditions. A boost converter can be added to this rectifier. This combination will improve the extracted power is lower than with the controlled rectifier (inverter) [11].

Since the early presented converter topologies for PMSG based VSWT have several drawbacks, such us high complexity of dual LCL DC/AC converter [19] or insufficient voltage regulation capability of the isolated buck type converter with the uncontrolled rectifier [10], the new topology of the interfacing converter with the HF isolation transformer for PMSG based VSWT systems is presented in this paper. The topology presented has good voltage regulation capabilities at a relatively simple power circuit.

Challenges of PMSG based VSWT

This section introduces the properties of wind energy, emphasizing wind energy extraction by means of PMSG based VSWT. Operation modes of VSWT with fixed blades are analyzed and generator characteristics are given.

Wind turbine characteristics

Equation (1) gives the total power available in the wind, where A is the rotor area, ρ is the air density and v is the wind velocity.

$$(1) \quad P_m = 0.5\rho Av^3$$

Only a part of the total wind energy can be extracted. The available energy part in wind is described by the power coefficient C_p . The theoretical maximum value of this coefficient is 0.59 and it is called the Betz limit [7].

$$(2) \quad P_{turbine} = 0.5C_p\rho Av^3$$

The practical values of C_p lie between 0.4 and 0.5 for industrial wind turbines [7]. This power coefficient is a function of the tip-speed ratio λ . An example of this function is shown in Fig. 2. The tip-speed ratio shows the relation between the circumferential velocity of the blade tips and the wind velocity:

$$(3) \quad \lambda = \frac{r\Omega}{v}$$

where: r – is the rotor radius, Ω – is the angular rotor speed.

Rotors are usually designed so that power coefficient C_p has the maximum values at the speed ratio in the range from 4 to 8.

Since the coefficient C_p is the function of the tip-speed ratio the power extracted by the wind turbine depends on the wind velocity and the rotational speed. Power curves at different wind velocities for turbines with fixed blade position are shown in Fig. 3.

Fig. 3 indicates that the maximal power can be captured from wind turbines only if they are of a variable speed type. This figure illustrates also another feature of variable speed turbines: generator's speed is four times lower at the cut-in wind speed than at the rated velocity.

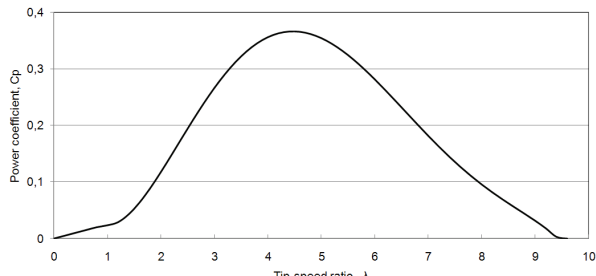


Fig.2. Power coefficient C_p vs. tip-speed ratio

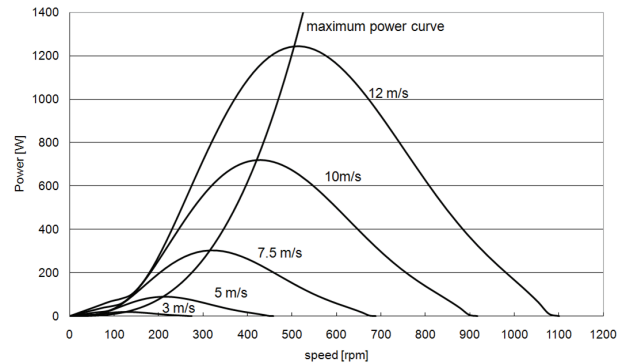


Fig.3. VSWT power vs. rotation speed of turbine at different wind velocities

The wind velocity determines the rotational speed of the wind turbine and the generator. Since it has direct impact on power converter operation modes, an example of wind velocity distribution at 10 meter height is shown in Fig. 4, but the corresponding energy yield in Fig. 5.

Three distinct operating modes of the variable speed wind turbine generator can be emphasized: slow speed, rated speed and high speed. Slow speed occurs when the wind velocity lies in the range from 3m/s till 7m/s, rated speed - 7...8 m/s and high speed mode is at higher velocities. This division of modes is made according to the normalized energy yield (Fig. 5). The rated speed corresponds to wind velocity with maximum energy.

These distributions are characteristic of Baltic coastal regions and so can be used as reference for interface converter design. The distribution of wind velocity per wind turbine modes is presented in Table 1. It shows that the wind turbine is silent one quarter of the time and half of the time works at low speed.

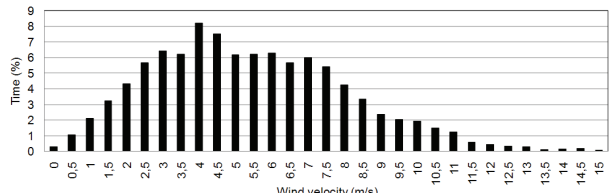


Fig.4. An example of wind velocity distribution

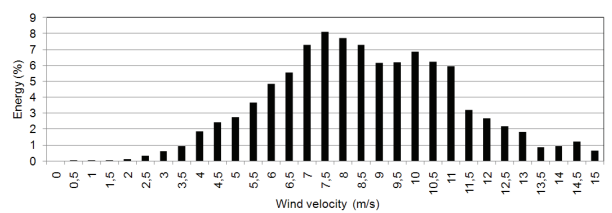


Fig.5. An example of normalized energy yield

Table 1. Wind turbine modes

Parameter \ Mode	No speed	Slow speed	Rated speed	High speed
Wind velocity range [m/s]	0 – 3	3.5 – 6.5	7 – 8	8.5 – 25
Time	23%	46%	16%	15%
Energy	0%	22%	24%	54%

PMSG based wind turbine

PMSG based VSWTs have three distinct operation modes: silent mode, variable speed operation mode and constant speed mode. A turbine is silent in two cases: wind speed is below a cut-in level or above the cut-off speed. If the speed is below its cut-in level it produces

insufficient torque to move the turbine. At the same time winds above the cut-off level may damage the turbine that must be stopped at such conditions. A turbine usually starts to operate at 3 m/s and it should be stopped at the wind speed above 25 m/s [7]. Turbines operate at variable speed in the wind velocity range from cut-in to rated wind speed. Rated wind speed differs by turbine types, but often has the value of 12 meters per second. Constant speed mode takes place above the rated wind speed. Turbine output power remains constant at this mode (Fig. 6).

PMSGs with 8 pole pairs are considered as a power source in this research. Its line voltage is 140V at 375 rpm, but it can operate up to 510 rpm. This speed is considered as the maximum power operational point for the turbine and the generator. Generator power reaches 1250W at this point, but the output voltage is 183V. Cut-in speed for a turbine is 125 rpm and it can produce 40W, but the generator voltage is only 48V at this point. So this is the lowest input voltage for a converter. Generator speed and voltage characteristics are shown in Fig. 7.

Topologies of interface converter for PMSG based VSWT

Interface converter for a PMSG based VSWT can have different topologies. Topologies with HF isolation for VSWT application already known are studied in this section to evaluate their pros and cons in the context of the described PMSG utilization in such systems and a new interface converter topology with qZS DC/DC converter based HF isolation is offered. There are only few converter topologies with high frequency isolation for small wind applications studied in the literature [10,15]. In [10] the authors have proposed a buck type isolated DC/DC converter.

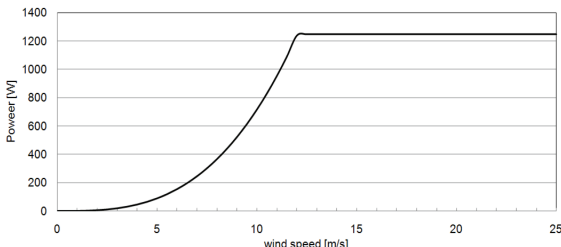


Fig.6. Output power of VSWT

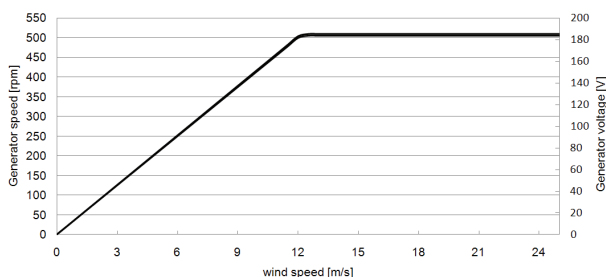


Fig.7. Generator speed and voltage vs. wind speed

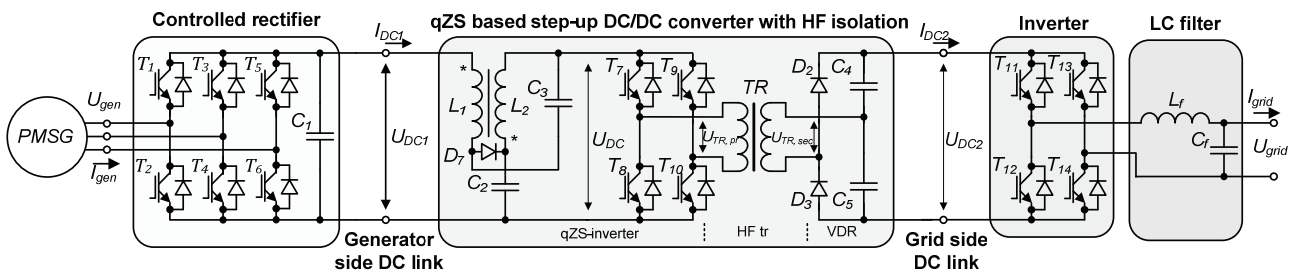


Fig.8. Power circuit of the proposed interface converter

Variable generator voltage is rectified with a three-phase diode bridge firstly into proportional DC voltage. Stabilization of the main drawback of this solution is high currents in the transformer's primary winding at rated wind speeds that will the grid side DC link voltage is obtained with the buck type isolated DC/DC converter by means of duty cycle variation. reduce converter efficiency at this operating point. In [15] the authors have proposed a one-phase soft-switched dual LCL DC/AC converter. This converter utilizes a controlled rectifier for generator voltage rectification and DC link voltage stabilization. The soft-switched dual LCL DC/AC converter needs stable DC link voltage, so generator voltage should be boost up to its maximum voltage amplitude value in the whole input voltage range that will reduce the efficiency of the controlled rectifier at low generator speed.

To improve the efficiency of the PMSG based VSWT system a new converter topology is introduced, presented in Fig. 8. It consists of a three-phase full bridge controlled rectifier (generator side inverter) with PFC functionality and a quasi-Z-source (qZS) DC/DC converter with an HF transformer for galvanic isolation. Grid side inverters with output filters are not discussed here.

A PFC inverter converts the variable voltage with variable frequency U_{gen} from the PMSG into a stabilized DC voltage U_{DC1} . The qZS DC/DC converter offers galvanic isolation and voltage level adjustment by means of the transformation coefficient. The unique qZS impedance network and appropriate control offer an additional voltage regulation capability at high efficiency. Stabilized DC link voltage U_{DC2} can be inverted into the grid current by an appropriate inverter.

Operating principle of the new interface converter

This research attempts to prove the ability of the proposed topology to ensure stable grid side DC link voltage U_{DC2} . For this reason only the operating principles of the controlled rectifier and the qZS DC/DC converter will be studied in more detail. The power circuit of the qZS based DC/DC converter is shown in Fig. 8 and operation modes in Fig. 9. The voltage boost necessary is obtained by two steps. The PFC rectifier stabilizes the generator side DC link voltage U_{DC1} to a 150V level when the generator voltage is below 112V. The DC link voltage U_{DC1} has the following relation with the generator line voltage U_{gen} in the PFC mode:

$$(4) \quad U_{DC1} = \frac{U_{trp-p} \cdot U_{gen} \cdot \sin \omega t}{\sqrt{3} \cdot U_r \cdot \sin \omega t}$$

where: U_{trp-p} – is the sawtooth voltage, U_r – is the value of the reference signal amplitude.

The controlled rectifier works as a usual rectifier when the generator voltage U_{gen} is above 112V. In this mode the DC link voltage is changed proportionally to the generator voltage, at the range from 150V in rated speed conditions up to 250V at the maximal speed.

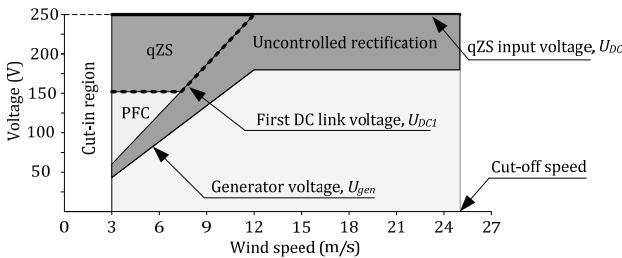


Fig.9. Operation modes of the proposed interface converter

The qZS based HF isolation converter is stabilizing the qZS-inverter input voltage U_{DC} to 250V despite the voltage variations on the generator side DC link. The stabilized input voltage U_{DC} ensures inverter operation with the fixed duty cycle, thus ensuring constant volt second balance of the isolation transformer. The input voltage U_{DC} regulation is obtained by changing the shoot-through duty cycle [20].

The input voltage U_{DC} and the first DC link voltage U_{DC1} have the following relation:

$$(5) \quad U_{DC} = \frac{U_{DC1}}{1 - 2 \cdot D_S}$$

where: D_S - is the shoot-through duty cycle.

The shoot-through duty cycle is zero when the first DC link voltage U_{DC1} is equal to the necessary input voltage U_{DC} . In such cases the qZS-inverter operates without shoot-through states.

Analysis of simulation and experimental results

Simulations of the controlled rectifier and the qZS DC/DC converter at different operation modes were performed to prove the functionality of the proposed topology. PSIM software was used for these simulations. Lossless models of the controlled rectifier and the qZS DC/DC converter were developed for the required simulations. Parameters of the developed models of experimental setup are summarized in Table 2.

Table 2. General specifications of the experimental setup

Component	Value or type
<i>PMSC</i>	
Phase resistance	1 Ω
Phase inductance	5 mH
<i>Interface converter</i>	
$T_1 \dots T_6$	600 V/48 A IGBT (IXSH24N60AU1)
$T_7 \dots T_{10}$	600 V/12 A IGBT (G4PC30UD)
D_I	600 V/120 A fast diode (STTH200L06TV)
D_2, D_3	1.2 kV/60 A FRED (DSEI2x61-12B)
Capacitance of C_1	470 μF
Inductance of L_1 and L_2	1.2 mH
Capacitance of C_2 and C_3	60 μF
HF transformer turns ratio	1: 1.2
Capacitance of C_4 and C_5	25 μF

Simulation of the controlled rectifier was performed at three different operating modes: minimum generator voltage, edge of PFC operation and maximum speed conditions, taking into account available power. Fig. 10 illustrates controlled rectifier's ability to boost up generator voltage in cut-in speed conditions.

Generator current is no more sinusoidal when the generator voltage U_{gen} reaches 112V (Fig. 10), but is not so distorted as in the case of pure rectifier operation (Fig. 11). Rectifier simulation results shows that the voltage of the first DC link is kept in predefined limits in all generator operation modes.

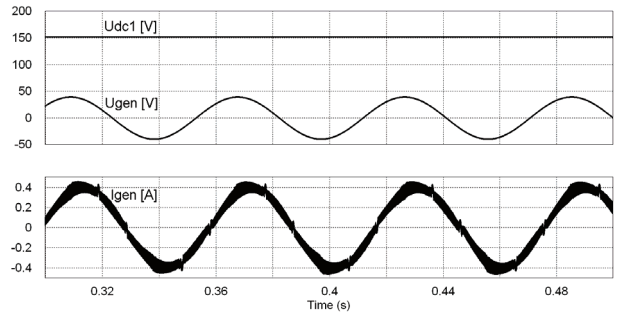


Fig.10. Generator current I_{gen} and rectifier output voltage U_{DC1} at $U_{gen} = 48V$

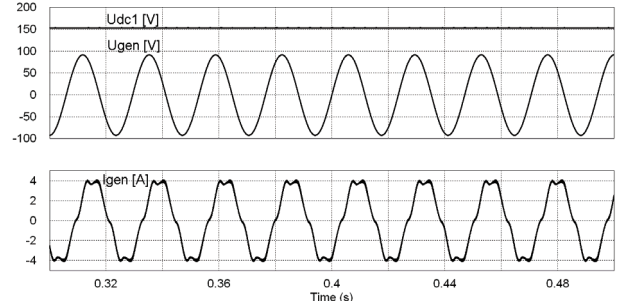


Fig.11. Generator current I_{gen} and rectifier output voltage U_{DC1} at $U_{gen} = 112V$

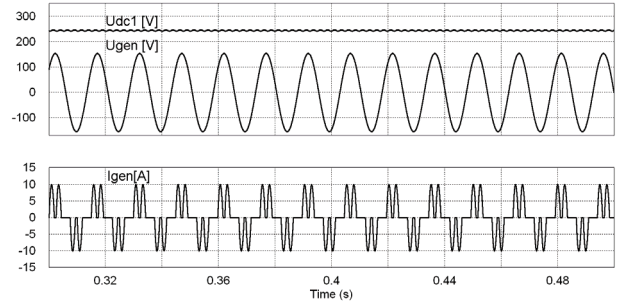


Fig.12. Generator current I_{gen} and rectifier output voltage U_{DC1} at $U_{gen} = 183V$

Simulations of the qZS DC/DC converter with the voltage doubler rectifier were performed at two different modes. The first simulation was made in the rated conditions – the generator side DC link voltage U_{DC1} was 150V and the load of the voltage doubler rectifier was 330W. The generator side DC link and the qZS inverter input voltage are shown in Fig. 13. It can be seen that the qZS inverter input voltage has pulsations caused by shoot through states, but amplitude is higher than first DC link voltage. As active state is shifted away from shoot-through state, an amplitude voltage is attached to transformer.

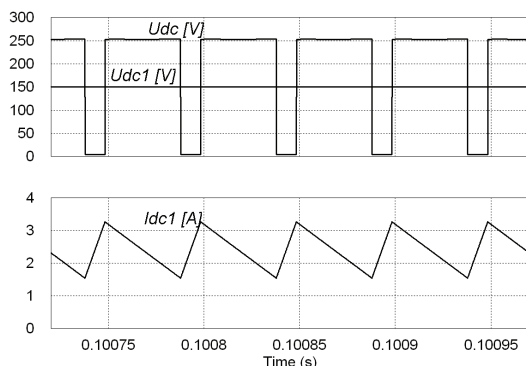


Fig.13. Voltage and current of qZSi at rated conditions

The second simulation was performed at the maximum generator voltage and 1250W load at the voltage doubler rectifier output. The qZS network input voltage U_{DC1} matches the qZS inverter voltage U_{DC} in these conditions and there is no need for voltage boost. The qZS inverter input voltage U_{DC} has small ripple due to the high transformer current (Fig.14).

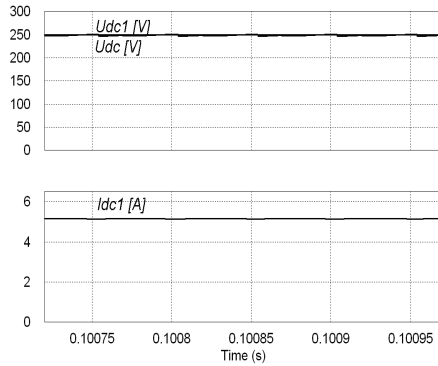


Fig.14. Voltage and current of qZSi at maximum power conditions

Experiments with the controlled rectifier were performed to ensure that there is no need for additional inductors between the PMSG and the rectifier for proper boost functionality. The first test was performed at the generator voltage $U_{gen} = 48$ V and 40 W load, which corresponds to the cut-in speed conditions. Simple boost control was realized by controlling only three lower transistors with a fixed duty cycle at 10 kHz switching frequency. Due to this, simplified control generator current I_{gen} (Fig. 15a) is not sinusoidal. Note that the apparent amplitude of the generator voltage in this figure U_{gen} (150 V) is not equal to the actually generated one because the generator is loaded - periodically tied to the DC link voltage U_{DC1} (Fig. 15b).

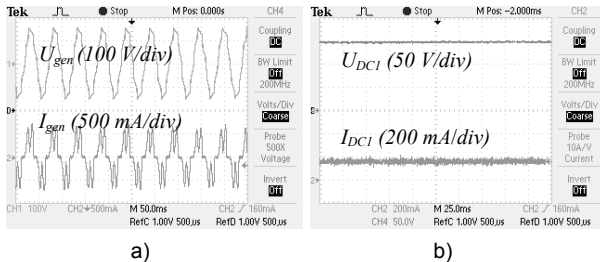


Fig.15. PMSM voltage and current (a) and generator side DC link voltage and current (b) at 40 W

The second test was performed at rated speed conditions, with the generator speed at 315 rpm and turbine power at 330 W. At this point the amplitude of the generator voltage U_{gen} is 150 V and boost control are not needed (Fig. 16).

The third test was performed at maximal speed and power of the PMSG: 510 rpm and 1250 W, respectively (Fig. 17). Since the nominal speed of the generator is

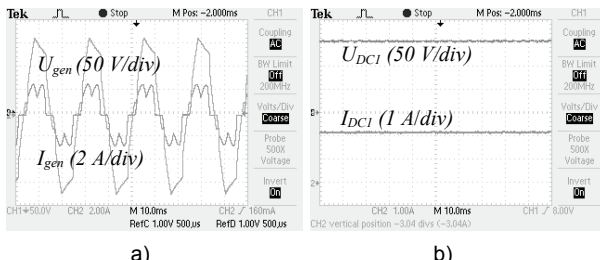


Fig.16. PMSM voltage and current (a) and generator-side DC link voltage and current (b) at 330 W

375 rpm, it was required to verify the generator's ability to produce the power necessary at that speed. The amplitude of the generator's output voltage reaches 250 V at this point and is maximal input voltage for the qZS based step-up DC/DC converter.

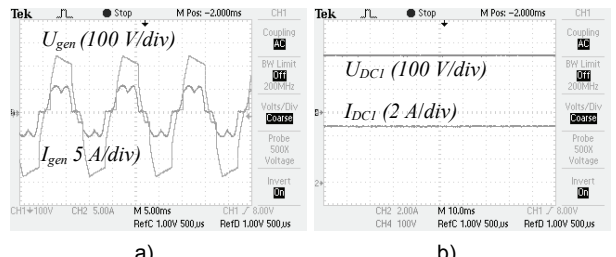


Fig.17. PMSM voltage and current (a) and generator-side DC link voltage and current (b) at 1250 W

To verify the overall performance of the qZS based step up DC/DC converter three experiments were performed at different power levels and corresponding voltages. The PWM shoot-through control technique [19] was implemented during the tests. The qZS network was operating at 20 kHz frequency, but isolation transformer at 10 kHz.

In the first test the generator-side DC link voltage was set to 150 V that corresponds to the cut-in and rated wind speed conditions. The load that corresponds to the turbine power at cut-in is 40 W. The qZS based DC/DC converter operates in the discontinuous conduction mode (DCM) at such load. (Fig. 18) Due to long current paths in the laboratory prototype of the qZS based DC/DC converter that leads to parasitic inductances, the voltage oscillations can be observed at zero input current intervals.

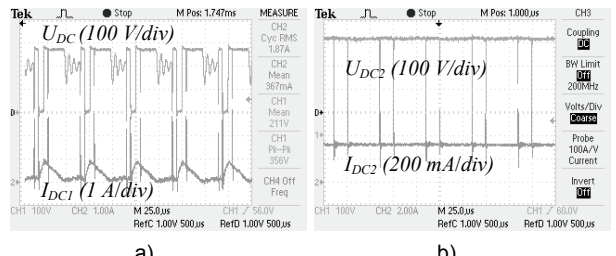


Fig.18. Voltage and current waveforms of the qZS based step-up DC/DC converter at 40 W: intermediate DC link voltage and input current (a), grid side DC link voltage and output current (b).

The second test was performed at the same generator-side DC link voltage ($U_{DC1} = 150$ V), but power was raised to 330 W that corresponds to turbine power at the rated wind speed. To boost the input voltage to the desired voltage level of the intermediate DC-link (250 V) the shoot-through duty cycle D_S was set to 0.2. Fig. 19a shows that the qZSI operates in the CCM, thus ensuring the demanded gain of the input voltage. Moreover, the voltage doubler rectifier provides the demanded grid side DC-link voltage level ($U_{DC2} = 405$ V) (Fig. 19).

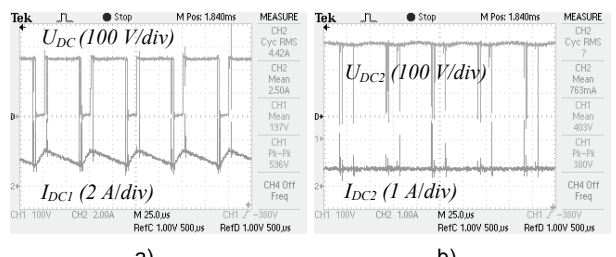


Fig.19. Voltage and current waveforms of the qZS based step-up DC/DC converter at 330 W: intermediate DC link voltage and input current (a), grid side DC link voltage and output current (b)

The third test was performed at the maximum generator-side DC link voltage ($U_{DC1} = 250$ V), which corresponds to the maximal power of the turbine (1250 W). At this operating point, when the input voltage equals the desired intermediate DC-link voltage ($U_{DC1} = U_{DC} = 250$ V), the shoot-through states were eliminated ($D_S = 0$) and the converter operated as a traditional VSI (Fig. 20). In that case the isolation transformer is supplied with voltage pulses with the amplitude value equal to the generator-side DC link voltage.

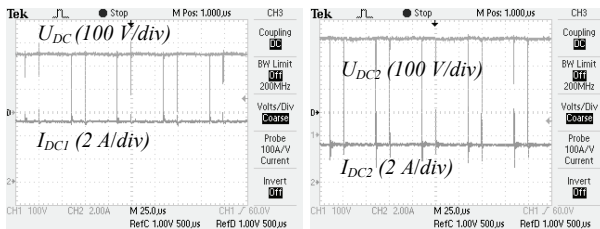


Fig.20. Voltage and current waveforms of the qZS based step-up DC/DC converter at 1250 W: intermediate DC link voltage and input current (a), grid side DC link voltage and output current (b).

Acknowledgments to be inserted at the end of the article using type size 9 and Arial italic.

Conclusions

The study of the wind theory shows that a VSWT allows maximum power from air flow to be extracted. PMSG based VSWT characteristics and wind properties on the Baltic coastal regions were analyzed to define the converter operation modes. Analysis of the converter topologies studied earlier shows that they are not well suited for VSWT applications due to the high complexity of the parallel LCL DC/AC converter or low efficiency in the case of the isolated buck type converter.

For these reasons the new topology of PMSG based VSWT and grid interfacing converter is presented in this paper.

Simulations of the converter were performed to verify its ability to ensure necessary output voltage at all modes.

In order to verify theoretical assumptions the 1.3 kW laboratory prototype of the proposed converter was elaborated and tested.

The test results show that the PWM rectifier can ensure the required level of the generator side DC link voltage $U_{DC1} = 150$ V at the unity power factor in its input in that mode. The qZS-based DC/DC converter with high frequency isolation offers additional voltage boost properties to the interface converter. The tests of the qZS-based DC/DC converter demonstrate its proper operation in all input voltage and power ranges. It operates in the DCM mode at the cut-in condition that enhances its boost properties, but in the CCM at higher power.

This research work has been supported by Estonian Ministry of Education and Research (Project SF0140016s11) and Estonian Science Foundation (Grant ETF8538).

REFERENCES

- [1] Cristina L. Archer and Mark Z. Jacobson. Evaluation of global wind power, 2005. Journal Of Geophysical Research, Vol. 110
- [2] World wind energy association. World Wind Energy Report 2009. [online]. available: http://www.wwindea.org/home/images/stories/worldwindenergyreport2009_s.pdf
- [3] Requirements for the connection of micro-generators in parallel with public low-voltage distribution networks, EN 50438:2007
- [4] Tan, K.; Islam, S. "Optimum control strategies in energy conversion of PMSG wind turbine system without mechanical sensors" IEEE Transactions on Energy Conversion, vol.19, no.2, pp. 392- 399, June 2004.
- [5] Arifujaman, M.; Iqbal, M.T.; Quaicoe, J.E.; "A comparative study of the reliability of the power electronics in grid connected small wind turbine systems," Canadian Conference on Electrical and Computer Engineering, 2009. CCECE '09, pp.394-397, 3-6 May 2009
- [6] Yogesh M.; Kawale Mtech; Subroto Dutt; "Comparative study of Converter Topologies used for PMSG Based Wind Generation", Second International Conference on Computer and Electrical Engineering, Dubai, UAE, 2009, pp. 367-371
- [7] Manfred Stiebler. Wind Energy Systems for Electric Power Generation. Berlin: Springer-Verlag Berlin Heidelberg, 2008
- [8] Anderson, J., Peng, F.Z., "Four Quasi-Z-Source Inverters", 2008 IEEE Power Electronics Specialist Conference, PESC 2008, Rhodes, Greece, 2008, pp. 2743-2749
- [9] Yanto, H.A.; Chun-Ta Lin; Jong-Chin Hwang; Sheam-Chyun Lin; "Modeling and control of household-size vertical axis wind turbine and electric power generation system," International Conference on Power Electronics and Drive Systems, 2009. PEDS 2009., pp.1301-1307, 2-5 Nov. 2009
- [10] Derbyshire, J.; Nayar, C.V. "Modelling, simulation and testing of grid connected small scale wind systems," Australasian Universities Power Engineering Conference, 2007. AUPEC 2007, pp.1-6, 9-12 Dec. 2007
- [11] Pathmanathan, M.; Tang, C.; Soong, W.L.; Ertugrul, N.; "Comparison of power converters for small-scale wind turbine operation," Australasian Universities Power Engineering Conference, 2008. AUPEC '08, pp.1-6, 14-17 Dec. 2008
- [12] Yanto, H.A.; Chun-Ta Lin; Jong-Chin Hwang; Sheam-Chyun Lin; "Modeling and control of household-size vertical axis wind turbine and electric power generation system," International Conference on Power Electronics and Drive Systems, 2009. PEDS 2009. pp.1301-1307, 2-5 Nov. 2009
- [13] Fujin Deng; Zhe Chen; , "Power control of permanent magnet generator based variable speed wind turbines," International Conference on Electrical Machines and Systems, 2009. ICEMS 2009, vol. pp.1-6, 15- 18 Nov. 2009
- [14] S. Zhang, K.-J. Tseng, D.M. Vilathgamuwa, T.D. Nguyen, X.-Y. Wang, "Design of a robust grid interface system for PMSG-based wind turbine generators," IEEE Transactions on Industrial Electronics, vol. 58, no. 1, pp. 316-328, Jan. 2011
- [15] Li, X.; Bhat, A.; "Multi-cell operation of a high-frequency isolated DC/AC converter for grid-connected wind generation applications," International Conference on Industrial and Information Systems (ICIIS), 2009, pp.169-174, 28-31 Dec. 2009
- [16] Dehghan, S.M.; Mohamadian, M.; Varjani, A.Y.; "A New Variable-Speed Wind Energy Conversion System Using Permanent-Magnet Synchronous Generator and Z-Source Inverter," IEEE Transactions on Energy Conversion , vol.24, no.3, pp.714-724, Sept. 2009.
- [17] Arifujaman, M.; Iqbal, M.T.; Quaicoe, J.E.; "A comparative study of the reliability of the power electronics in grid connected small wind turbine systems," Canadian Conference on Electrical and Computer Engineering, 2009. CCECE '09, pp.394-397, 3-6 May 2009
- [18] Shchur, I.; "Impact of nonsinusoidalness on Efficiency of alternative electricity generation systems," International School on Nonsinusoidal Currents and Compensation (ISNCC), 2010, pp. 218-223, June 2010
- [19] Vinnikov, D.; Roasto, I.; Zakis, J.; Strzelecki, R.; "New Step-up DC/DC Converter for Fuel Cell Powered Distributed Generation: Some Design Guidelines", Przeglad Elektrotechniczny, 86 pp. 245-252.

Authors: Dr. Sc. techn. Dmitri Vinnikov, Principal Research Fellow, Tallinn University of Technology, Ehitajate str. 5, 19086 Tallinn, Estonia, E-mail: dmitri.vinnikov@ieee.org; Dr. Sc. ing. Lauris Biseneks, Head of doctoral studies department, Riga Technical University, Kalku1, LV-1658, Riga, E-mail: lauris.biseneks@rtu.lv; Dr. Sc. ing. Ilya Galkin, Professor, Riga Technical University, Kronvalda Boulevard 1, LV-1010, Riga, E-mail: ilja.galkins@gmail.com.